Electric Field Detection Using an Electro-optic Polymer Refilled Silicon Slot Photonic Crystal Waveguide

Xingyu Zhang[1],*, Amir Hosseini[2], Harish Subbaraman[2], Shiyi Wang[3], Qiwen Zhan[3], Jingdong Luo[4], Alex K.-Y. Jen[4], and Ray T. Chen[1],*

[1]*Microelectronics Research Center, Electrical and Computer Engineering Department, University of Texas at Austin, Austin, TX, 78758, USA*
[2]*Omega Optics, Inc, 8500 Shoal Creek Blvd, Bldg 4, Ste 200, Austin, TX 78757, USA*
[3] *Department of Electrical and Computer Engineering, University of Dayton, Dayton, OH 45469, USA*
[4] *Department of Materials Science and Engineering, University of Washington, Seattle, Washington 98195, USA*
**Corresponding author: xzhang@utexas.edu, raychen@uts.cc.utexas.edu, Tel:512- 471-4349, Fax: +1-512-471-8575*

Abstract: We demonstrate an integrated photonic electric field sensor based on an electro-optic polymer refilled silicon slot photonic-crystal waveguide modulator driven by a bowtie-antenna. The minimum detectable electric field is measured to be 2.5V/m at 8.4GHz.

OCIS codes: (280.4788) Optical sensing and sensors; (130.5296) Photonic crystal waveguides; (130.4110) Modulators

Electromagnetic field (EMF) sensors have shown promising applications in electromagnetic pulse detection, process control, RF IC testing, and so on [1]. Traditional electronic EMF sensors have large conductive probes which perturb the field to be measured and also make the device bulky. To address these problems, integrated photonic EMF sensors have been developed, in which an optical signal is modulated by an RF signal collected by a small enough antenna [1]. Such photonic devices have a few inherent advantages over conventional electronic sensors, such as compact size, high sensitivity, broad bandwidth, and noise immunity. In this paper, we design and demonstrate a compact, sensitive and broadband integrated photonic EMF sensor based on bowtie antenna coupled silicon-organic hybrid (SOH) slot photonic crystal waveguide (SPCW) modulator. Slow-light effects in the electro-optic (EO) polymer refilled silicon SPCW [2], together with broadband electric field enhancement provided by the bowtie antenna, are utilized to enable an ultra large effective in-device EO coefficient (r_{33}) over 1000pm/V [3]and thus high sensitivity.
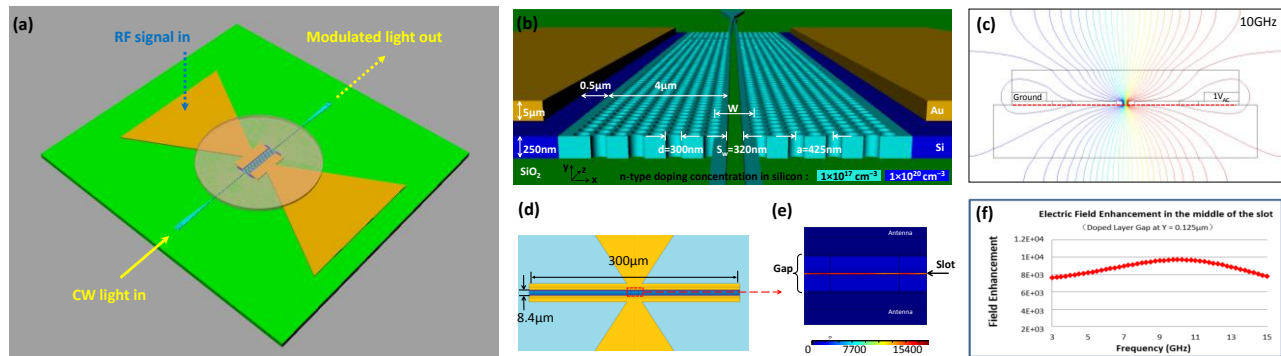

Fig. 1. (a) Schematic view of the key part of the electromagnetic field sensor consisting of an EO polymer refilled slot PCW phase modulator and a bowtie antenna. An external arm is combined with this phase modulator to form a MZI structure, converting phase modulation to intensity modulation. (b) Tilted view showing the cross section of the antenna-coupled slot PCW, with two-level n-type silicon doping. (c) Cross-sectional view of RF (10GHz) electric potential distribution across the doped silicon slot PCW. (d) and (e) Enhanced electric field distribution inside the antenna feed gap. (f) Electric field enhancement factor inside the slot versus RF frequency.

Fig. 1 (a) shows a schematic of the photonic EMF sensor. EO polymer SEO125 (r_{33}=125pm/V) is used to refill the 300μm-long silicon SPCW with a slot width (S_w) of 320nm on SOI substrate [4]. A strip- to slot-waveguide mode converter [5] is designed to efficiently couple light from input strip waveguide into the slot PCW. The bowtie antenna is used as a receiving antenna, driving electrodes, and poling electrodes. The bowtie antenna collects incident electric field, transforms it into high power density electric field within its feed gap, and directly modulates the phase of optical CW signal propagating along the EO polymer refilled SPCW embedded within the feed gap. For measurement, we convert this phase modulation to intensity modulation using an external arm enabled MZI structure. In this way, the amplitude of an incident EMF is characterized by measuring the intensity of the modulated optical signal.

In order for our sensor to operate in GHz regime, the top silicon layer is selectively ion implanted with P+ at the concentration of 1×10^{17}cm^{-3} and 1×10^{20}cm^{-3}, as shown in Fig. 1 (b), to reduce the PCW resistivity and thus the RC time delay [6]. Effective medium approximations are to calculate effective silicon resistivity and effective silicon RF dielectric constant. Fig. 1 (c) shows the simulated cross-sectional view of the RF electric potential distribution (1V$_{AC}$, 10GHz) across the device, showing over 90% of voltage drops inside the slot. With bow arm length of 3mm and flare angle of 60°, the bowtie antenna has a central resonant frequency at 10GHz. Figs. 4 (d) and (e) show the simulated electric field uniformly enhanced in the PCW

slot. Fig. 4 (f) shows the simulated spectrum of field enhancement (FE), defined as resonant electric field divided by incident electric field. The electric field inside the slot is enhanced by a maximum factor of 10,000 at 10GHz.

The silicon photonic circuitries are fabricated using e-beam lithography, photolithography, RIE, and ion implantation, while gold electrodes are patterned by photolithography and electroplating. A microscope image of the fabricated MZI is shown in the inset of Fig. 2 (a). Next, the EO polymer is infiltrated into the slot and holes of silicon PCW region by spincoating, and the device is poled by an electric field of 100V/μm at 145 °C. The peak leakage current density is $1.4 \times 10^{-6} A/m^2$, which is comparable to that measured in a thin film configuration ($2.36 \times 10^{-6} A/m^2$ in data sheet), showing that the 320nm-wide slot dramatically reduces leakage current and increases poling efficiency [7].
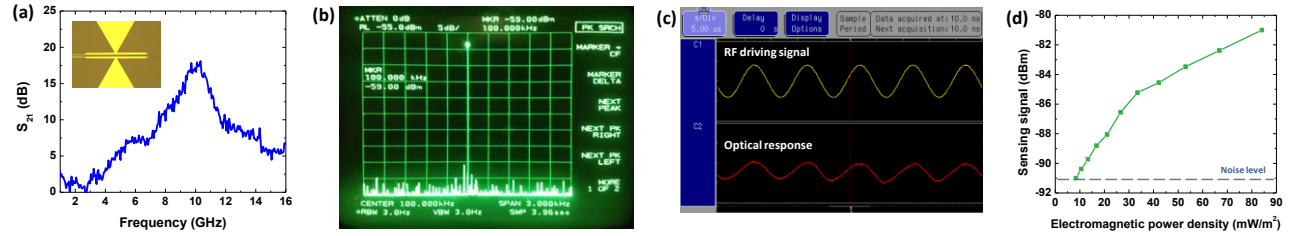

Fig. 2. (a) Measured S21 parameter of the broadband bowtie antenna. The inset shows a top-view microscope image of the fabricated device. (b) The EO modulation response signal as measured on the MSA. (c) EO modulation transfer function. (d) The measured sensing signal as a function of electromagnetic power density at 8.4GHz.

In order to demonstrate the GHz broadband characteristics of the bowtie antenna, a network analyzer is used to measure the S_{11} of the bowtie antenna. Assuming negligible loss, the S_{21} is inferred from the measured S_{11} as shown in Fig. 2 (a) with broadband response. The peak response at 10GHz agrees well with the simulated peak field enhancement at 10GHz in Fig. 1 (f). This result indicates that our sensor can be used to detect the electromagnetic field over a broad frequency bandwidth in GHz regime. Next, an EO modulation experiment is performed. 1556nm TE-polarized light is coupled to a MZI system formed by a 90/10 f splitter, a 50/50 fiber combiner and a variable optical attenuator (VOA), in which our device is in one arm while the VOA on the other arm. A sinusoidal RF signal with V_{pp}=1V at 100KHz is directly applied across the two bows. Modulated optical output is collected by a photodetector and measured by a microwave spectrum analyzer (MSA) [8], as shown in Fig. 2 (b). The modulation transfer function measured by a logic analyzer is shown in Fig. 2 (c). This low-frequency EO modulation experiment demonstrates the successful poling of EO polymer and the functionality of MZI which is then used in the next EMF sensing experiment.

In the EMF sensing experiment, an RF signal at 8.4GHz from a sweep oscillator is fed into a horn antenna (Gain G_t=6dB) which is placed at R=30cm vertical distance above the sensor. The horn antenna works as a transmitting antenna and the bowtie antenna on the sensor works as a receiving antenna. The sensing signal is measured by the MSA, similar to the measurement in the previous EO modulation experiment. Next, the RF power applied on the horn antenna (P_t) is tuned, corresponding to the variation of EMF power density near the sensor based on Eq. 1.

$$S_{avg} = G_t P / 4\pi R^2 \tag{1}$$

where S_{avg} is the average Poynting vector. The measured sensing signal v.s. EMF power density is plotted in Fig. 2 (d). When the EMF power density decreases to 8.4mW/m², the sensing signal is below noise level. Based on Eq. 2, this minimum detectable EMF power density is used to estimate the minimum detectable electric field as 2.5V/m at 8.4GHz, considering the EMF has a predominantly plane-wave character within the far-field region of horn antenna.

$$|E| = \sqrt{2 S_{avg} / \varepsilon_o \varepsilon_r c} = 2.5 V/m \tag{2}$$

where ε_0=8.85$\times 10^{-12}$F/m, $\varepsilon_r \approx 1$ is, c=3$\times 10^8$m/s. Details can be seen in Ref [9].

Reference

[1] V. Passaro, et al, "Electromagnetic field photonic sensors," *Progress in quantum electronics,* vol. 30, pp. 45-73, 2006.
[2] X. Zhang, et al, "Polymer-based Hybrid Integrated Photonic Devices for Silicon On-chip Modulation and Board-level Optical Interconnects."
[3] X. Zhang, et al, "Demonstration of Effective In-device r33 over 1000 pmV in Electro-optic Polymer Refilled Silicon Slot Photonic Crystal Waveguide Modulator," in *CLEO: Science and Innovations*, 2013, p. CTu2F. 6.
[4] X. Zhang, et al, "Wide optical spectrum range, subvolt, compact modulator based on an electro-optic polymer refilled silicon slot photonic crystal waveguide," *Optics letters,* vol. 38, pp. 4931-4934, 2013.
[5] X. Zhang, et al, "Highly Efficient Mode Converter for Coupling Light into Wide-slot Photonic Crystal Waveguide," Optics Express, 2014 (Under review).
[6] X. Zhang, et al, "Electric field sensor based on electro-optic polymer refilled silicon slot photonic crystal waveguide coupled with bowtie antenna," in *SPIE OPTO*, 2013, pp. 862418-862418-8.
[7] X. Zhang, et al, "Highly Linear Broadband Optical Modulator Based on Electro-Optic Polymer," *Photonics Journal, IEEE,* vol. 4, pp. 2214-2228, 2012.
[8] C.-Y. Lin, et al, "High dynamic range electric field sensor for electromagnetic pulse detection," *Opt. Exp,* vol. 19, pp. 17372-17377, 2011.
[9] X. Zhang, et al, "Integrated Photonic Electromagnetic Field Sensor Based on Broadband Bowtie Antenna Coupled Silicon Organic Hybrid Modulator," *Lightwave Technology, Journal of,* vol. PP, pp. 1-1, 2014.